Vol 16 No 4, April 2007
1009-1963/2007/16(04)/1008-06

Chinese Physics

© 2007 Chin. Phys. Soc.
and IOP Publishing Ltd

Calculation of photon angular distribution and polarization for radiative recombination for high-charged hydrogen-like ions*

Shen Tian-Ming(沈天明)[a)b)], Chen Chong-Yang(陈重阳)[a)b)†], and Wang Yan-Sen(王炎森)[a)b)]

[a)] *The Key Laboratory of Applied Ion Beam Physics, the Ministry of Education, Shanghai* 200433, *China*
[b)] *Shanghai Electron Beam Ion Trap Laboratory, Modern Physics Institute, Fudan University, Shanghai* 200433, *China*

(Received 9 June 2006; revised manuscript received 4 August 2006)

In this paper a systematic study is carried out on the angular distribution and polarization of photons emitted following radiative recombination of H-like ions by a non-relativistic dipole approximation. In order to incorporate the screening effect due to inner-shell electrons, a distorted wave approach is used. The dependences of the calculated angular distribution and polarization on the reduced energy and nuclear charge are fitted by the corresponding empirical formulas respectively.

Keywords: radiative recombination, angular distribution, polarization, fit formula
PACC: 3480L

1. Introduction

The study of radiative recombination (RR) is important in application to inertial confinement fusion and for understanding fundamental physics in astrophysics plasmas.[1,2] In addition, RR is also important for the process of cooling an ion beam in a storage ring with electrons.[3] In the electron beam ion trap (EBIT), different radiative strengths are determined by normalizing those x-ray intensities to the RR x-ray intensity using theoretical RR cross section.[4] High resolution spectroscopy of emitted photons has offered new possibilities to study state selective RR for bare and few electron ions.[5,6] For the experimental study of detecting the radiation, it is worthwhile to know not only the RR cross section, but also the angular distribution and polarization of the emitted radiation. However, there are few studies on the angular distribution and polarization of the photons produced by the RR process.

The earliest analytical formula of RR cross sections for the bare ion target was originally derived by Kramers by using a semiclassical approach.[7] The Kramers formula has frequently been used to evaluate the RR cross section because of its simplicity. The RR cross section can be treated in the non-relativistic dipole approximation given by Hahn[8] and Burgess[9] for arbitrary (n, l) states. In the case of the ions with a few electrons, an effective charge method has been adopted to approximately treat the screening effect.[8,10] The comparison of Kramers formula with the exact calculation shows that it is accurate within 5% for higher n ($n \geq 20$) and within 20% for lower n states.[11] Some relativistic treatments were given by Lee and Pratt,[12] Kim and Pratt,[13] Ichihara,[14] and Zeng *et al.*[15] In Ref.[14], the comparison of the calculated RR cross section for bare ion target by relativistic treatment including all multipole contribution with those from non-relativistic dipole approximation shows that for nuclear charge $Z \leq 50$ and incident electron energy $E_{\rm i} \leq 10\,{\rm keV}$, the discrepancy between relativistic cross section and the non-relativistic cross section increases with the increase of incident energy and nuclear charge number, and the maximum relative deviation is about 10%. In Ref.[15], the relativistic effects and the multipole contribution of the photoionization processes are discussed for highly charged ions. The calculation shows that the multipole contribution could be omitted when the incident electron energy is lower than 50 keV.

In 1989, Scofield reported relativistic theoretical studies of the photon angular distribution and polarization in recombination of selected highly charged ions, Ba^{46+} and Ni^{26+}, using electrons with a few

*Project supported by the National Science Foundation of China (Grant Nos 10574029 and 10434050), the Chinese Association of Atomic and Molecular Data and National High-Tech ICF Committee in China.
†Corresponding author. E-mail: chychen@fudan.edu.cn (C.Y. Chen)

kilo electron volts of energy.[16] Later on, Pajek and Schuch reported the non-relativistic calculations on the photon angular distribution and polarization of RR for bare ions at very low energy in the storage ring experiments.[5]

Regarding that the cross section for RR into $2p$ orbital is large and the photon following the RR process is not completely polarized, in this work we calculate the cross sections and anisotropy parameters for RR into the $2p$ orbital for hydrogenlike isoelectronic sequence: Ne^{9+}, Si^{13+}, Ar^{17+}, Ti^{21+}, Fe^{25+}, Ni^{27+}, Se^{33+}, Kr^{35+}, Zr^{39+} and Mo^{41+} by using the non-relativistic dipole approximation, with relativistic corrections and a distorted wave approach. From our earlier works, Refs.[17] and [18], we can see that the distorted wave method reflects reasonably the variation of screening effect due to inner-shell electrons of target ions with incident electron energy in contrast with the pure Coulomb method. By using this method, the calculated cross sections and anisotropy parameters for some ions agree well with other theoretical calculation and experiments. Based on the calculations of the cross sections and anisotropy parameters, the photon angular distribution and polarization of the emitted photons following the RR process can be obtained. In many studies, it is necessary to obtain the data quickly and accurately. The dependences of the calculated angular distribution and polarization on the reduced energy u and nuclear charge Z are fitted by the corresponding empirical formulae. The reduced energy is defined as $u = E_\mathrm{i}/I_{2p}$, where E_i is the incident electron energy and I_{2p} is the ionization potential of $2p$ orbital. The energy range in our calculation is from $u = 0.1$ to $u = 6$ as required for non-relativistic dipole approximation.

2. Theoretical method

In the non-relativistic dipole approximation, the RR cross section is given in units of πa_0^2 by[10,17]

$$\sigma_{nl} = \frac{2(2l+1)-q}{2(2l+1)} \frac{16}{3\sqrt{2}\alpha^2} \left(\frac{\hbar\omega}{mc^2}\right)^3 \left(\frac{mc^2}{E_\mathrm{i}}\right)^{1/2} \times \left[l(R_{nl}^{E_\mathrm{i},l-1})^2 + (l+1)(R_{nl}^{E_\mathrm{i},l+1})^2\right], \quad (1)$$

where q is the number of electrons presented in the subshell (n,l) of the target ion before capture, α is the fine structure constant, $\hbar\omega$ is the emitting photon energy, m is the mass of electron, and the bound-free dipole matrix is given by

$$R_{nl}^{E_\mathrm{i},l'} = \int_0^\infty R_{E_\mathrm{i},l'} R_{nl} r \mathrm{d}r, (l' = l \pm 1), \quad (2)$$

where R_{nl} is the bound state radial wave function calculated by Cowan's atom-structure programs in the HFR (Hartree–Fock approximation with relativistic correction) method[19] and $R_{E_\mathrm{i},l'}$ is the continuum state radial wavefunction based on distorted wave approximation.[20] The total RR cross section is then given by

$$\sigma^{\mathrm{RR}} = \sum_{nl} \sigma_{nl}, \quad (3)$$

where σ_{nl} are summed over the open shells.

Rate coefficient $\langle\nu\sigma\rangle$ for RR can be obtained from

$$\langle v\sigma\rangle = \sum_{nl}^{n_{\max}} \int \sigma_{nl}(v) v f(v,t) \mathrm{d}v, \quad (4)$$

where $n_{\max}$ is the maximum primary quantum number in the calculation, $f(v,T)$ is the distribution function of relative velocity. Usually, $f(v,T)$ is represented by the Maxwell distribution for plasma at the temperature T as

$$f(v,T) = \left(\frac{m}{2\pi kT}\right)^{3/2} \mathrm{e}^{-mv^2/2kT}. \quad (5)$$

The differential RR cross section into a specific state, describing the angular distribution of the emitted photon, can be expressed in non-relativistic dipole approximation in terms of the RR cross section σ_{nl} as[5,16]

$$\frac{\mathrm{d}\sigma_{nl}(\theta,\varphi)}{\mathrm{d}\Omega} = \frac{\sigma_{nl}}{4\pi}\left[1 + \frac{1}{2}\beta_{nl}(3\sin^2\theta\cos^2\varphi - 1)\right], \quad (6)$$

where θ is the angle between the directions of the photon wave vector $\boldsymbol{k}$ and the incident electron momentum $\boldsymbol{p}$, while φ is the angle between the polarization vector and the plane defined by $\boldsymbol{p}$ and $\boldsymbol{k}$ (see in Fig.1). The anisotropy parameter β_{nl} can be expressed as[5,18]

$$\beta_{nl} = \left[(l+2)(l+1)\left(R_{nl}^{E_\mathrm{i},l+1}\right)^2 + l(l-1)\left(R_{nl}^{E_\mathrm{i},l-1}\right)^2 - 6l(l+1)R_{nl}^{E_\mathrm{i},l+1}R_{nl}^{E_\mathrm{i},l-1}\cos(\delta_{l+1} - \delta_{l-1})\right] \cdot \left\{(2l+1)\left[(l+1)\left(R_{nl}^{E_\mathrm{i},l+1}\right)^2 + l\left(R_{nl}^{E_\mathrm{i},l-1}\right)^2\right]\right\}^{-1}, \quad (7)$$

where δ_{l+1} is the phase shift of the distorted wave and is numerically determined by using the asymptotic behaviour of the wavefunction. The degree of polarization is given by

$$P_{nl}(\theta) = \frac{I_{//}(\theta) - I_{\perp}(\theta)}{I_{//}(\theta) + I_{\perp}(\theta)}, \tag{8}$$

where $I_{//}(\theta)$ and $I_{\perp}(\theta)$ are the radiation intensities associated with electric vector in ($\varphi = 0°$) and perpendicular ($\varphi = 90°$) to the $(\boldsymbol{p}, \boldsymbol{k})$ plane respectively. Since $I_{//,\perp}(\theta) \sim \mathrm{d}\sigma_{nl}/\mathrm{d}\Omega$, the degree of polarization can be obtained from Eq.(3) and Eq.(5) as

$$p_{nl}(\theta) = \frac{3\beta_{nl}\sin^2\theta}{2(2-\beta_{nl}) + 3\beta_{nl}\sin^2\theta}. \tag{9}$$

From Eq.(7), it can be seen that for recombination into s state, $\beta_{n0} = 2$, the photons are completely linearly polarized with an electric vector in the $(\boldsymbol{p}, \boldsymbol{k})$ plane, and for the higher (n, l) states, the photons are no longer completely polarized and the polarization is strongest at $\theta = 90°$.

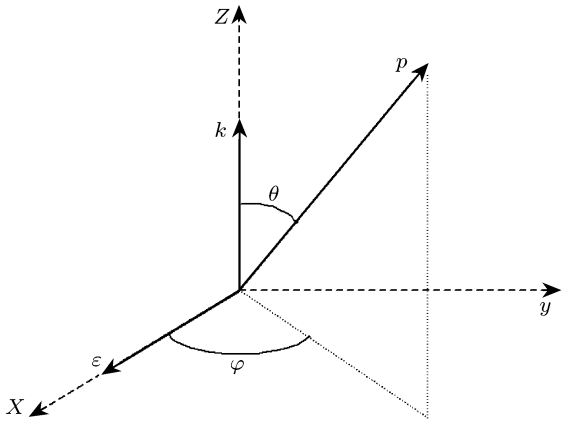


Fig.1. The coordinate system used to describe the RR process, $\boldsymbol{p}$ is the momentum of the incident electron, $\boldsymbol{k}$ is the direction of the photon, and $\boldsymbol{\varepsilon}$ is the unit vector along the photon electronic vector for the photon polarization.

3. Results and discussions

3.1. Cross sections for radiative recombination

We have calculated cross sections for RR into $2p$ orbital of ten H-like ions: Ne^{9+}, Si^{13+}, Ar^{17+}, Ti^{21+}, Fe^{25+}, Ni^{27+}, Se^{33+}, Kr^{35+}, Zr^{39+} and Mo^{41+}. Figure 2 shows the dependences of the cross sections for RR into $2p$ orbital of two H-like ions, Ti^{21+} and Mo^{41+}, on the reduced energy u. The cross sections for Ti^{21+} are the lowest and the cross sections for Mo^{41+} are the highest one among the cross sections of all the ten ions. The largest relative deviation between these two curves is 12% at $u = 6$. So we can easily fit the dependence of all the cross sections on the reduced energy u and nuclear charge Z by an empirical formula.

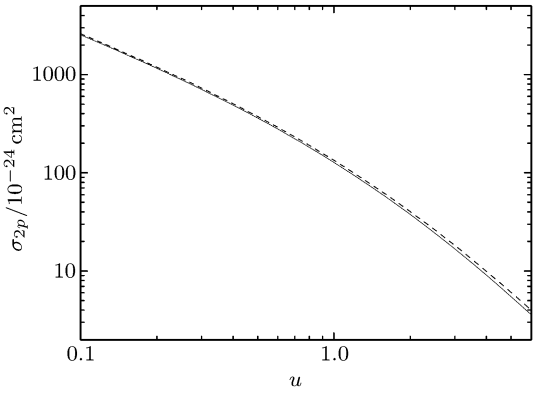


Fig.2. Cross sections for RR into $2p$ orbital are plotted as a function of u. Solid: Ti^{21+}; dash line: Mo^{41+}.

In Fig.3, the solid curves denote the dependences of calculated RR rate coefficient for Fe^{25+} with Maxwell distribution. In this calculation, $n_{\max} = 70$, and the rate coefficients for $n \geq 20$ are obtained from the Kramers semiclassical formula with $Z = 25.5$. For comparison, we also show the corresponding values computed from rate coefficients given by Arnaud and Raymond[21] using photoionization cross sections obtained by Clark *et al*[22] with Hartree–Fock wavefunctions and by Verner and Ferland[23] with the Hartree–Dirac–Slater and R-matrix method. From Fig.3, it can be seen that the relative deviation between our calculated values and other theoretical results is within about 10%.

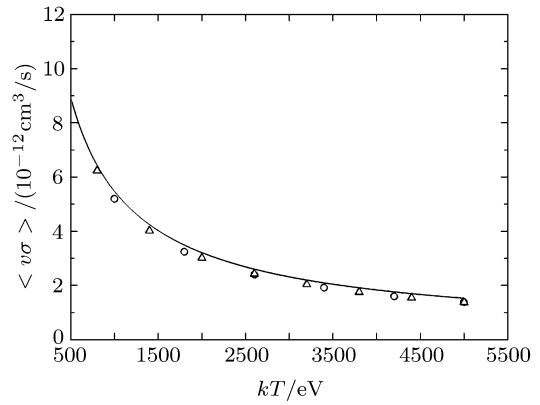


Fig.3. Dependence of rate coefficient for Fe^{25+}. Solid: the distorted wave method. The open circles are theoretical data from Ref.[21], and the open triangles are from Ref.[23].

3.2. Fit of cross sections for radiative recombination

We fit our calculation cross sections for ten H-like ions with the empirical formula as

$$\sigma_{2p}^{\rm fit}(u) = \frac{A_1}{(u^3 + A_2u^2 + A_3u)}, \quad (10)$$

where A_1, A_2 and A_3 are three adjustable parameters obtained by an 'optimal calculation method'.[24] The average deviation from fit is defined as

$$F(\%) = \sqrt{\frac{1}{N}\sum_{i=1}^{N}\left(\frac{\sigma_{2p}^{\rm fit}(u) - \sigma_{2p}(u)}{\sigma_{2p}(u)}\right)^2} \times 100. \quad (11)$$

Table 1 lists the fit parameters in Eq.(7) and the average deviations for ten ions respectively. The ionization potentials of $2p$ orbital for individual ions are also listed. It can be seen that the average deviations are less than 0.2%. In order to obtain an empirical formula that can be used to fit the dependence of the calculated cross sections on the reduced energy u and nuclear charge Z, we take the lowest fitted cross sections $\sigma_{2p}^{\rm fit}(\mathrm{Ti}^{21+})$ as a benchmark and then plus a corrected term relative to u and Z. Figure 4 shows the dependence of the relative deviations between the calculated cross sections for ten ions and the benchmark $\sigma_{2p}^{\rm fit}(\mathrm{Ti}^{21+})$ on u. Regarding that the relative deviation is nearly linear to the reduced energy and that the relative deviation nonlinearly increases with the increase of the departure of the nuclear charge from $Z = 22$, we can well fit the scale of cross sections by the following formula:

$$\sigma_{2p}^{\rm fit}(u, Z) = \frac{1729}{(u^3 + 6.401u^2 + 6.145u)} \times[1 + 3.46 \times 10^{-5}(Z - 22)^2(u + 2.65)] \times(10^{-24}\mathrm{cm}^2). \quad (12)$$

Table 1. Ionization potentials of $2p$ orbital I (Ryd)*, RR cross section fit parameters and average deviations for individual ions.

H-like ions	I/(Ryd)	$A_1/(10^{-24}\mathrm{cm}^2)$	A_2	A_3	F/%
Ne^{9+}	2.056×10	1.896×10^3	6.887	6.608	0.11
Si^{13+}	4.273×10	1.761×10^3	6.479	6.218	0.09
Ar^{17+}	7.297×10	1.729×10^3	6.408	6.136	0.09
Ti^{21+}	1.113×10^2	1.729×10^3	6.401	6.145	0.08
Fe^{25+}	1.578×10^2	1.759×10^3	6.483	6.243	0.10
Ni^{27+}	1.842×10^2	1.783×10^3	6.548	6.318	0.10
Se^{33+}	2.757×10^2	1.875×10^3	6.777	6.602	0.10
Kr^{35+}	3.104×10^2	1.917×10^3	6.884	6.730	0.10
Zr^{39+}	3.861×10^2	2.023×10^3	7.159	7.051	0.12
Mo^{41+}	4.272×10^2	2.094×10^3	7.366	7.270	0.14

*1 Ryd =13.60 eV.

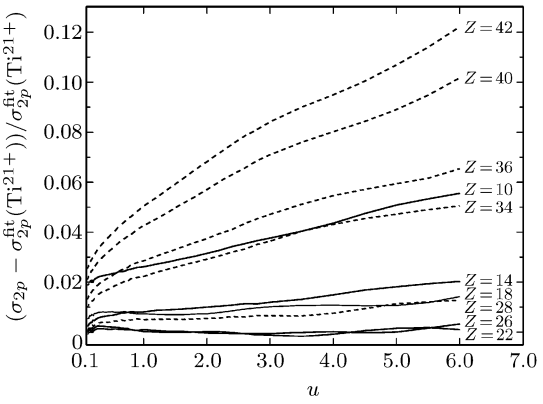


Fig.4. $(\sigma_{2p}(\mathrm{Ti}^{21+}) - \sigma_{2p}^{\rm fit}(\mathrm{Ti}^{21+}))/\sigma_{2p}^{\rm fit}(\mathrm{Ti}^{21+})$ is plotted as a function of u at the range from 0.1 to 6.

The largest deviation between the fitted cross sections from Eq.(12) and the calculated cross sections is about 1.0% when $10 \le Z \le 42$.

3.3. Calculation and fit of the anisotropy parameters

Figure 5 shows the anisotropy parameters β for RR into $2p$ orbital of five H-like ions: Si^{13+}, Ti^{21+}, Ni^{27+}, Kr^{35+} and Mo^{41+}. For the fit of the anisotropy parameters for individual ions, we use the empirical formula as

$$\beta^{\rm fit}(u) = B_1 + B_2\mathrm{e}^{-B_3u}, \quad (13)$$

where B_1, B_2, and B_3 are three adjustable parameters. (14)

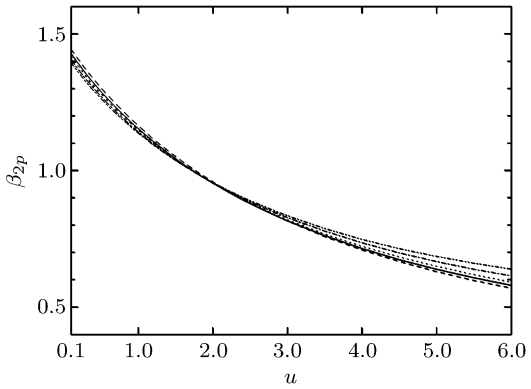


Fig.5. Anisotropy parameter is plotted as a function of u. Dashed: Si^{13+}; solid: Ti^{21+}; dotted: Ni^{27+}; dash-dotted: Kr^{35+}; dash-dot-dotted line: Mo^{41+}.

Table 2. Fit parameters for anisotropy parameter and average deviations for individual ions.

H-like ions	B_1	B_2	B_3	F/%
Ne^{9+}	0.4410	1.044	0.3434	0.49
Si^{13+}	0.4459	1.024	0.3453	0.48
Ar^{17+}	0.4539	1.006	0.3474	0.52
Ti^{21+}	0.4680	0.9851	0.3528	0.49
Fe^{25+}	0.4808	0.9652	0.3564	0.52
Ni^{27+}	0.4882	0.9544	0.3586	0.52
Se^{33+}	0.5125	0.9200	0.3663	0.52
Kr^{35+}	0.5241	0.9052	0.3714	0.50
Zr^{39+}	0.5463	0.8756	0.3796	0.45
Mo^{41+}	0.5622	0.8570	0.3892	0.44

Table 2 lists the fit parameters in Eq.(13) and the average deviations for individual ions respectively. It can be seen that almost all of the average deviations are less than 0.6%. In order to obtain an empirical formula that can be used to fit the dependence of the calculated anisotropy parameters on the reduced energy u and nuclear charge Z, we take the average of the fit parameters of all the ions, $B_{1,\mathrm{av}} = 0.4898, B_{2,\mathrm{av}} = 0.9554, B_{3,\mathrm{av}}(3) = 0.3582$, and then we take $\beta_{\mathrm{av}}(u) = 0.4898 + 0.9554\mathrm{e}^{-0.3582u}$ as a benchmark. Figure 6 shows the dependences of the relative deviations between the calculated anisotropy parameters for five ions and the benchmark β_{av} on u. It can be seen that curves are closest to one another when $u = 2.2$ and the values of β for Ni^{27+} are closest to the benchmark. So the scaled anisotropy parameters can be fitted by the following formula:

$$\beta^{\mathrm{fit}}(u, Z) = (0.4898 \times 0.9554\mathrm{e}^{-0.3582u}) \times [1 + 8.71 \times 10^4 (Z - 28)(u - 2.2)].$$

The largest deviation between the fitted anisotropy parameters from Eq.(14) and the calculated ones is within 2% when $14 \leq Z \leq 42$, and within 2.5% when $10 \leq Z \leq 4$.

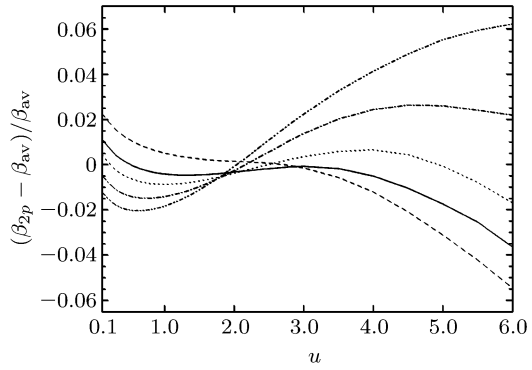


Fig.6. $(\beta_{2p} - \beta_{\mathrm{av}})/\beta_{\mathrm{av}}$ is plotted as a function of u at the range from 0.1 to 6. Dashed: Si^{13+}; solid: Ti^{21+}; dotted: Ni^{27+}; dash-dotted: Kr^{35+}; dash-dot-dotted line: Mo^{41+}.

3.4. Calculation and fit of photon angular distribution

Figure 7 shows the angular distribution of the emitted photon following the RR into $2p$ orbital for five ions when $u = 1$ and $\varphi = 0°$. Using Eqs.(6), (12) and (14), we can quickly calculate the angular distribution of the emitted photon for RR into $2p$ orbital of the H-like ions with $10 \leq Z \leq 42$.

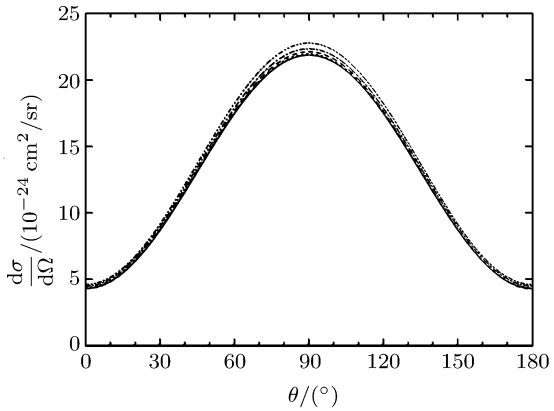


Fig.7. Photon angular distribution is plotted as a function of θ when $u = 1$. Solid: Ti^{21+}; dotted: Ni^{27+}; dashed: Si^{13+}; dash-dotted: Kr^{35+}; dash-dot-dotted line: Mo^{41+}, from bottom to top in Fig.7.

From the comparison of the fitted results and the calculated values for the angular distributions, we find that the deviation is about 1% when $14 \leq Z \leq 42$, and about 2% when $10 \leq Z \leq 14$.

3.5. Calculation and fit of photon polarization

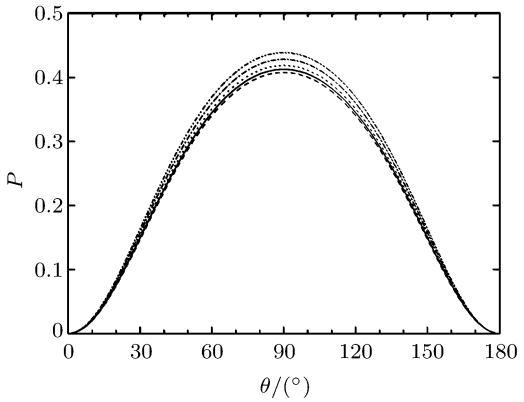


Fig.8. Photon polarization is plotted as functions of θ when $u = 5$. Dashed: Si^{13+}; solid: Ti^{21+}; dotted: Ni^{27+}; dash-dotted: Kr^{35+}; dash-dot-dotted line: Mo^{41+}, from bottom to top in Fig.8.

Figure 8 shows the polarization of the emitted photon for RR into $2p$ orbital of five ions when $u = 5$. Using Eqs.(9) and (14), we can quickly calculate the photon polarization for RR into $2p$ orbital of the H-like ions with $10 \leq Z \leq 42$.

From comparison of the fitted results and the calculated values for the polarizations, we find that the average deviation is about 2.5% when $14 \leq Z \leq 42$, and about 3% when $10 \leq Z \leq 14$.

4. Summary

In this paper, the cross sections, anisotropy parameters, photon angular distributions and photon polarizations for RR into $2p$ orbital of high-charged H-like ions with $10 \leq Z \leq 42$ are systematically calculated by using non-relativistic dipole approximation with relativistic corrections and a distorted wave approach. Our calculation agrees well with other theoretical calculations. Also, we present the empirical formulae and corresponding fit parameters for the dependence of all the calculated values on the reduced energy u and nuclear charge Z.

References

[1] Hahn Y 1997 *Rep. Prog. Phys.* **60** 691
[2] Stephens J A and Botero 1995-2000 *J. International Bulletin on Atomic and Molecular Data for Fusion* (Vienna: IAEA)
[3] Schuck R 1987 *Nucl. Instrum Methods* B **24-25** 11
[4] O'Rourke B E, Kuramoto H, Li Y M, Ohtani S, Tong X M, Watanabe H and Currell F J 2004 *J. Phys.* B **37** 2343
[5] Pajek M and Schuch R 1992 *Phys. Rev.* A **46** 6962
[6] Bosch F 1987 *Phys. Scr.* **36** 730
[7] Kramers H A 1923 *Philos. Mag.* **46** 836
[8] Hahn Y and Rule D W 1977 *J. Phys.* B **10** 2689
[9] Burgess A 1964 *Mem. R. Astron. Soc.* **69** 1
[10] McLaughlin D J and Hahn Y 1991 *Phys. Rev.* A **43** 1313
[11] Zerrad E and Hahn Y 1998 *J. Quant. Spectrosc. Radiat. Transfer.* **59** 637
[12] Lee C M and Pratt R H 1975 *Phys. Rev.* A **12** 1825
Lee C M and Pratt R H 1976 *Phys. Rev.* A **14** 990
[13] Kim Y S and Pratt R H 1983 *Phys. Rev.* A **27** 2913
[14] Ichihara A 2000 *At. Data Nucl. Data Tables* **74** 1
[15] Zeng S L, Pang J Q, Li P, Li Y M, Yan J and Wang J G 2005 *Acta Phys. Sin.* **54** 2625 (in Chinese)
[16] Scofield J H 1989 *Phys. Rev.* A **40** 3054
[17] Xia H N, Chen C Y, Shi X H, Qi J B and Wang Y S 2003 *Chin. Phys. Lett.* **20** 60
[18] Ou W Y, Shen T M, Chen C Y, Roger H and Zou Y M 2005 *Chin. Phys. Lett.* **22** 2248
[19] Cowan R D 1981 *The Theory of Atomic Structure and Spectra* (Berkeley, CA: University of California Press)
[20] Chen C Y, Qi J B, Wang Y S and Yang F J 2001 *At. Data Nucl. Data Tables* **79** 65
[21] Arnaud M and Raymond J 1992 *Astrophys. J.* **398** 394
[22] Clark R E H, Cowan R D and Bobrowicz F W 1986 *Atom. Data Nucl. Data Tables* **34** 415
[23] Verner D A and Ferland G J 1996 *Astrophys. J. Suppl. Series* **103** 467
[24] Xi S 1980 *The Optimal Calculation Method* (Shanghai: Shanghai Sci. Technol. Press) (in Chinese)